# SUPPORTING INFORMATION

# Aminolysis of Bis[bis(trimethylsilyl)amido]-Manganese, -Iron, and -Cobalt for the Synthesis of Mono- and Bis-Silylene Complexes

Zhiyuan He, Xiaolian Xue, Yilan Liu, Na Yu, Jeremy P. Krogman

## Table of Contents

# General information

Unless otherwise stated, all manipulations were performed under a nitrogen atmosphere using Schlenk techniques or in a Vigor glovebox maintained at or below 1 ppm of $O_2$ and $H_2O$. All new metal complexes were prepared and handled in the glovebox under $N_2$ atmosphere. $FeCl_2$, $CoCl_2$ and $MnCl_2$ were purchased from Strem chemical. $PhC(N^tBu)_2SiHCl_2$ (**1**),[1] $PhC(N^tBu)_2SiCl$ (**2**), $Li\{N(SiMe_3)_2\}(Et_2O)$,[1] $Fe\{N(SiMe_3)_2\}_2$,[2] $Co\{N(SiMe_3)_2\}_2$,[3] $Mn\{N(SiMe_3)_2\}_2$,[4] and 1,4-bis(2-bromophenyl)benzene[5] were synthesized by reported procedures. Other reagents were purchased from J&K Chemical and SCRC. Glassware was dried at 150 °C overnight. Celite and molecular sieves were dried at 200 °C under vacuum. Pentane, hexanes, and diethyl ether were degassed with nitrogen and dried by activated molecular sieves, and kept over 4 Å molecular sieves in a $N_2$-filled glovebox. NMR data were recorded on a Bruker 400 and 500 MHz, and are internally referenced to residual protio solvent signals (THF-$d_8$ (3.58, 1.72 ppm), $C_6D_6$ (7.16 ppm). Data for $^1$H NMR are reported as follows: chemical shift (δ ppm), multiplicity (s = singlet, d = doublet, t = triplet, m = multiplet, br = broad), IR data were recorded on a Thermo Scientific Nicolet iS5 FTIR. UV-vis spectra were recorded using a StellarNet BLACK Comet C-SR diode array miniature spectrophotometer connected to deuterium and halogen lamp by optical fiber using 1 cm matched quartz cuvettes at room temperature. Solution magnetic susceptibilities were determined by the Evans method.[6, 7] Elemental analysis was performed by the Analytical Laboratory of Shanghai Institute of Organic Chemistry (CAS). Several of the newly reported metal-halide compounds have elemental analysis results with low carbon values but matching nitrogen and hydrogen. The reported results are consistent for several samples and also consistent with some previously reported and related metal-halide containing complexes.[8-10]

X-ray crystallography:

Crystals were coated with Paratone-N oil and mounted on a Bruker D8 Venture diffractometer equipped with an APEX-II CCD diffractometer. The crystal was kept at 150 K during data collection. Using Olex2,[11] the structure was solved with the ShelXT[12] structure solution program using Intrinsic Phasing and refined with the XL[13] refinement package using Least Squares minimization.

# Experimental Procedure

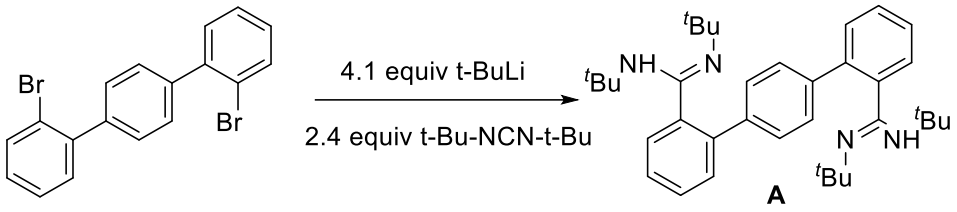


**Synthesis of 1,4-bis(2-(ditertbutylamidine)phenyl)benzene (A)**. A mixture of 1,4-bis(2-bromophenyl)benzene (0.9822 g, 2.53 mmol, 1 equiv) and diethyl ether (20 mL) in a Schlenk tube fitted with a screw-in Teflon stopper was frozen in a cold well, in an inert atmosphere glovebox. This mixture was allowed to thaw and *t*-BuLi solution (1.3 M in pentane, 8.18 mL, 4.2 equiv) was added rapidly via syringe while thawing. This yellow mixture was stirred for 30 min allowing it to reach room temperature. N,N'-Ditertbutylcarbodiimide (0.937 g, 6.07 mmol, 2.4 equiv) was added via syringe to the reaction mixture, which within minutes became a light-yellow solution. After stirring at room temperature for 3 h, 10 mL water was added to the mixture out of the glovebox. Volatiles were removed *via* rotary evaporation and the mixture was extracted with $CH_2Cl_2$ three times. The combined organic fractions were dried over $Na_2SO_4$, filtered, and the volatiles removed *via* rotary evaporation. 20 mL $CH_3CN$ was added to the grey solid and then the white solid product **A** (1.154 g, 85 %) was isolated after filtration. X-ray quality crystals were grown in $CH_3CN$ at 5 °C. Melting point: 213.7-214.6 °C. $^1$H NMR (500 MHz, $C_6D_6$) δ: 7.82 (d, 4H, Ar-*H*), 7.33 (d, 2H, Ar-*H*), 7.23 (d, 2H, Ar-*H*), 7.13 (m, 2H, Ar-*H*), 7.04 (t, 2H, Ar-*H*), 3.38 (d, 2H, N*H*), 1.42 (s, 18H, NH-C(C*H*$_3$)$_3$), 1.11 (d, 18H, C(C*H*$_3$)$_3$). $^{13}$C NMR (126 MHz, $C_6D_6$) δ: 149.97 (d), 140.26 (d), 139.46 (s),139.09 (t), 130.42 (s), 130.29 (s), 129.28 (s), 128.83 (s), 126.80 (s), 54.05 (s), 51.43 (s), 32.34 (d), 29.10(s). MS(m/z): calcd, 539.411 ($M^+$); found 539.411 (LC-MS, $M^+$).

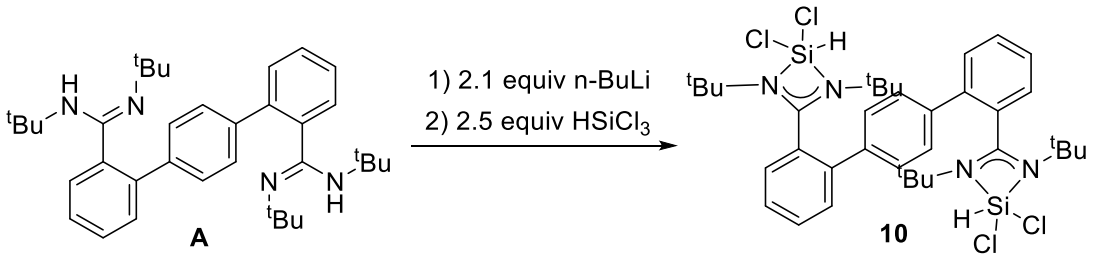


**Synthesis of 1,4-bis(2-(ditertbutylamidinate-dichlorosilane)phenyl)benzene (10).** A mixture of **A** (301.8 mg, 0.561 mmol, 1 equiv) and diethyl ether (5 mL) in a vial was frozen in a cold well. An *n*-BuLi solution (1.6 M in hexane, 0.7363 mL, 2.1 equiv) was added dropwise via syringe to the thawing solution of **A**. This yellow solution was stirred for 1 h allowing it to reach room temperature. A mixture of trichlorosilane (190 mg, 1.234 mmol, 2.5 equiv) and diethyl ether (5 mL) was added dropwise to the mixture, forming a white cloudy solution. After stirring at room temperature for 12 hours, the volatile materials were removed under reduced pressure and the residue was dissolved in toluene and filtered through Celite and a glass fiber paper. The toluene

solution was concentrated under reduced pressure and the product **10** (0.3788 g, 74%) was crystalized at -37 °C. Melting point: 217.5-219.5 °C. $^{1}$H NMR (500 MHz, $C_6D_6$) δ 7.85 (s, 4H, Ar-H), 7.29 (d, 2H, Ar-H), 7.03 (t, 2H, Ar-H), 6.90 (d, 2H, Ar-H), 6.78(s, 2H, Si-H), 1.12(s, 36H, Ar-H). $^{13}$C NMR (126 MHz, $C_6D_6$) δ: 170.52 (s), 138.94 (s), 138.37 (s), 131.22 (s), 130.94 (s), 130.01 (s), 129.57 (s), 129.47 (s), 127.01 (s), 56.11 (s), 30.96 (s). $^{29}$Si NMR (99 MHz, $C_6D_6$) δ -96.48. MS (m/z): calcd, 735.240 ($M^+$); found 735.236 (MS, $M^+$).

# $^{1}$H NMR Spectra

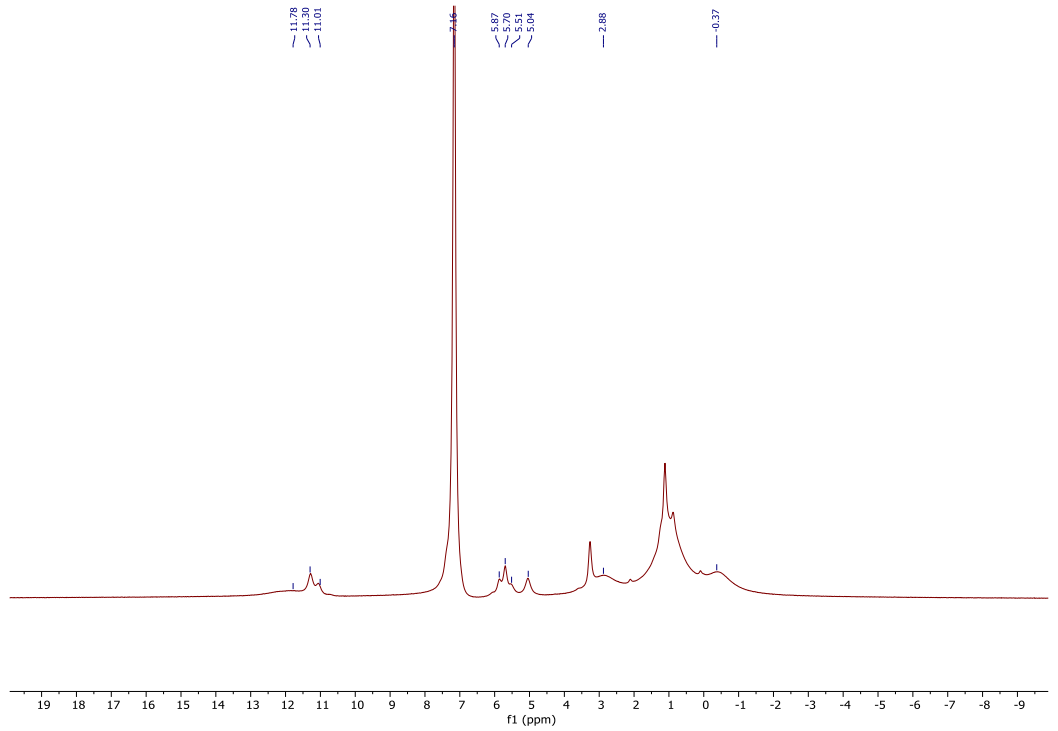


Figure S1. $^{1}$H NMR spectrum of {PhC(N$^{t}$Bu)$_2$SiCl}$_2$FeCl$_2$ (**3**) (400 MHz, $C_6D_6$).

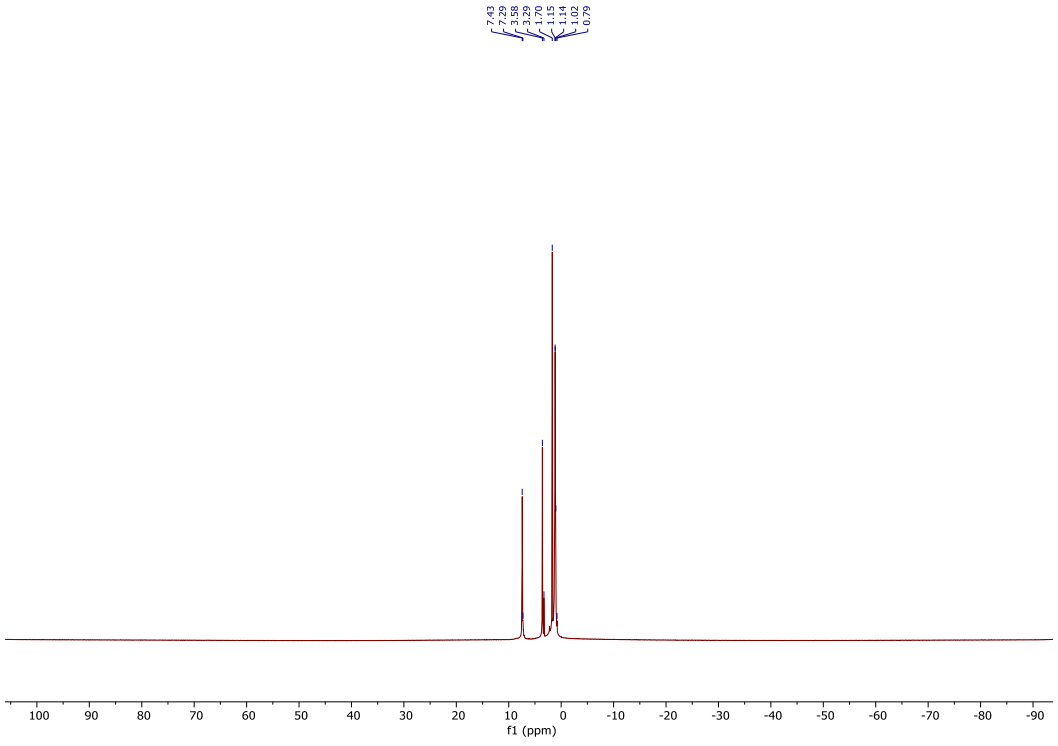


Figure S2. $^{1}$H NMR spectrum of {PhC(N$^{t}$Bu)$_2$SiCl}$_2$MnCl$_2$ (**4**) (500 MHz, THF-$d_8$).

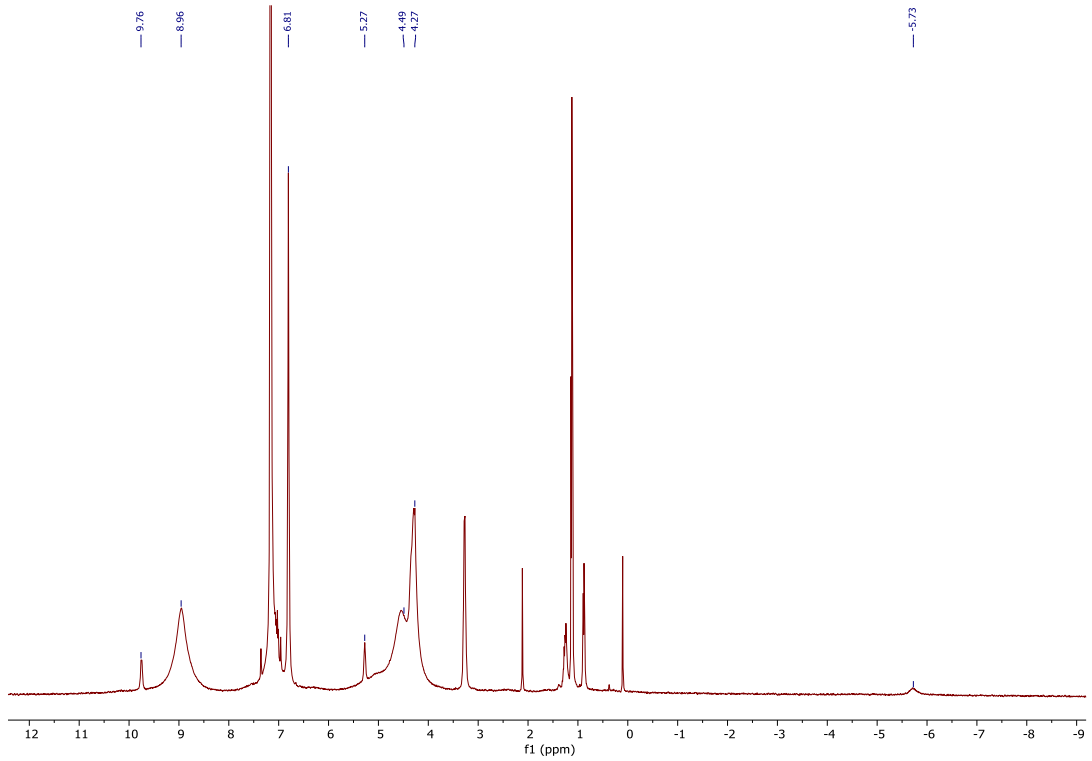


Figure S3. $^{1}$H NMR spectrum of [{PhC(N$^{t}$Bu)$_2$}Si{N(SiMe$_3$)$_2$}CoCl(μ-Cl)]$_2$ (**6**) (400 MHz, $C_6D_6$).

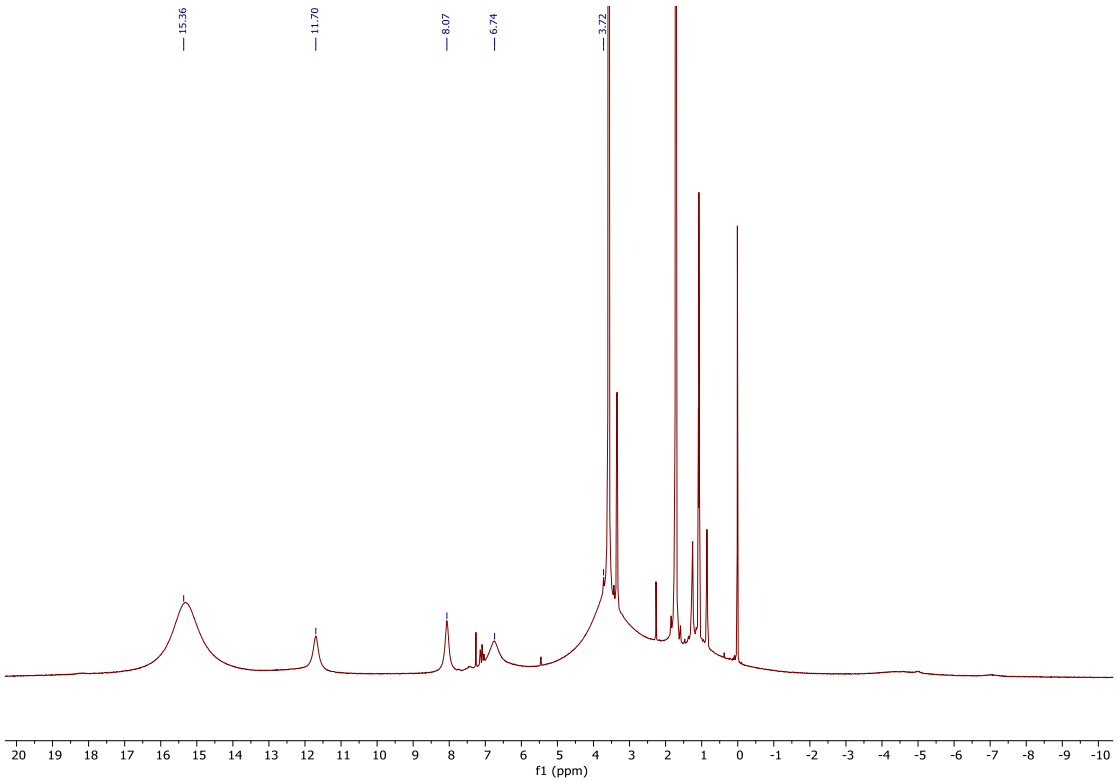


Figure S4. 1H NMR spectrum of [{PhC(NtBu)$_2$SiCl}Fe{N(SiMe$_3$)$_2$}(μ-Cl)]$_2$ (**7**) (500 MHz, THF-$d_8$).

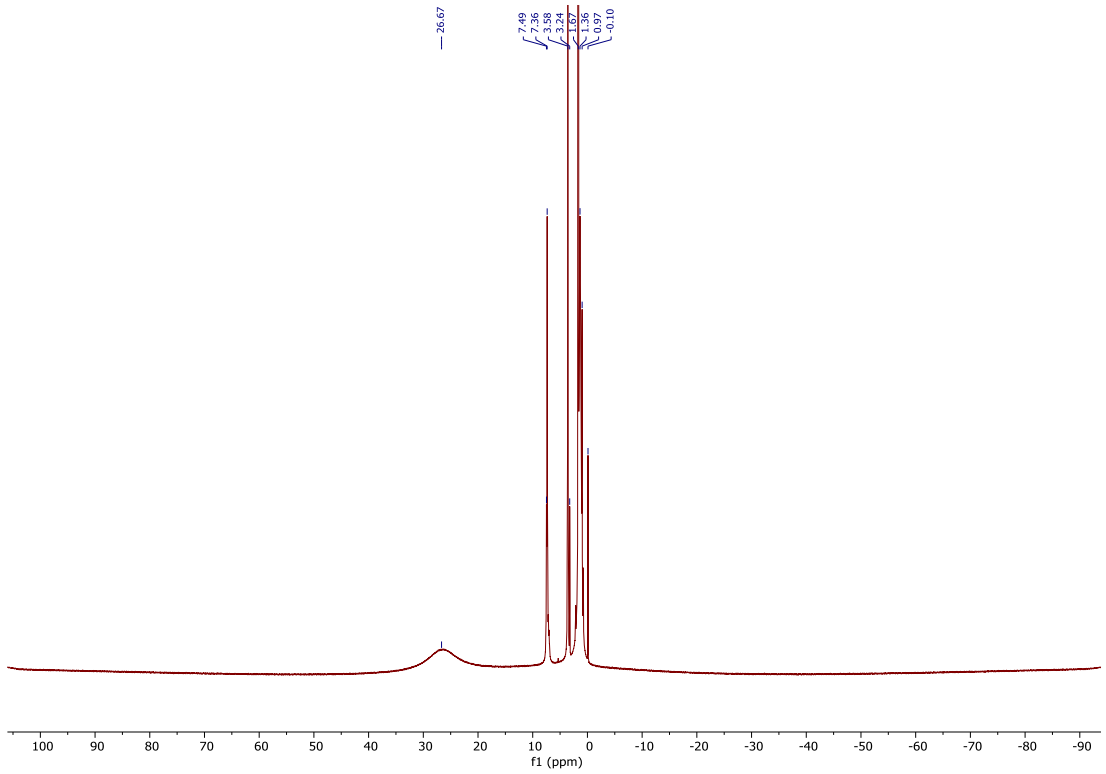


Figure S5. 1H NMR spectrum of [{PhC(NtBu)$_2$SiCl}Mn{N(SiMe$_3$)$_2$}(μ-Cl)]$_2$ (**8**) (500 MHz, THF-d$_8$).

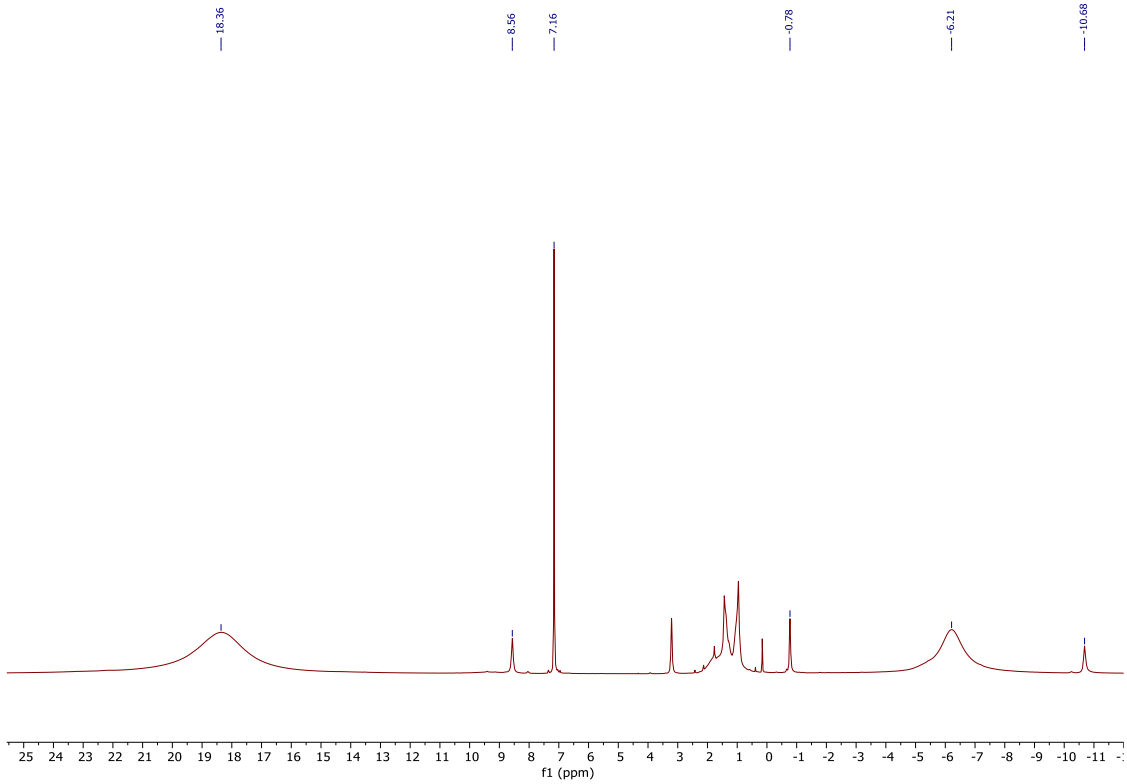

Figure S6. $^{1}$H NMR spectrum of {PhC(N$^{t}$Bu)$_2$SiCl}Fe{N(SiMe$_3$)$_2$}$_2$ (**9**) in $C_6D_6$

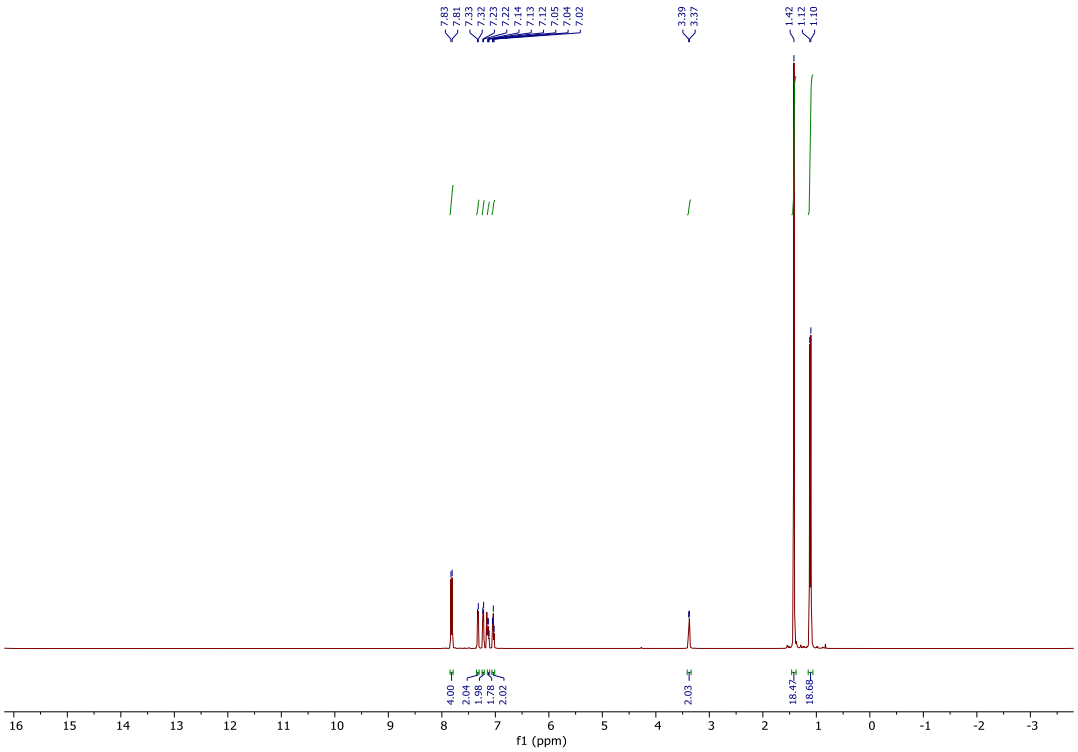


Figure S7. $^{1}$H NMR spectrum of 1,4-bis(2-(ditertbutylamidine)phenyl)benzene (**A**) in $C_6D_6$.

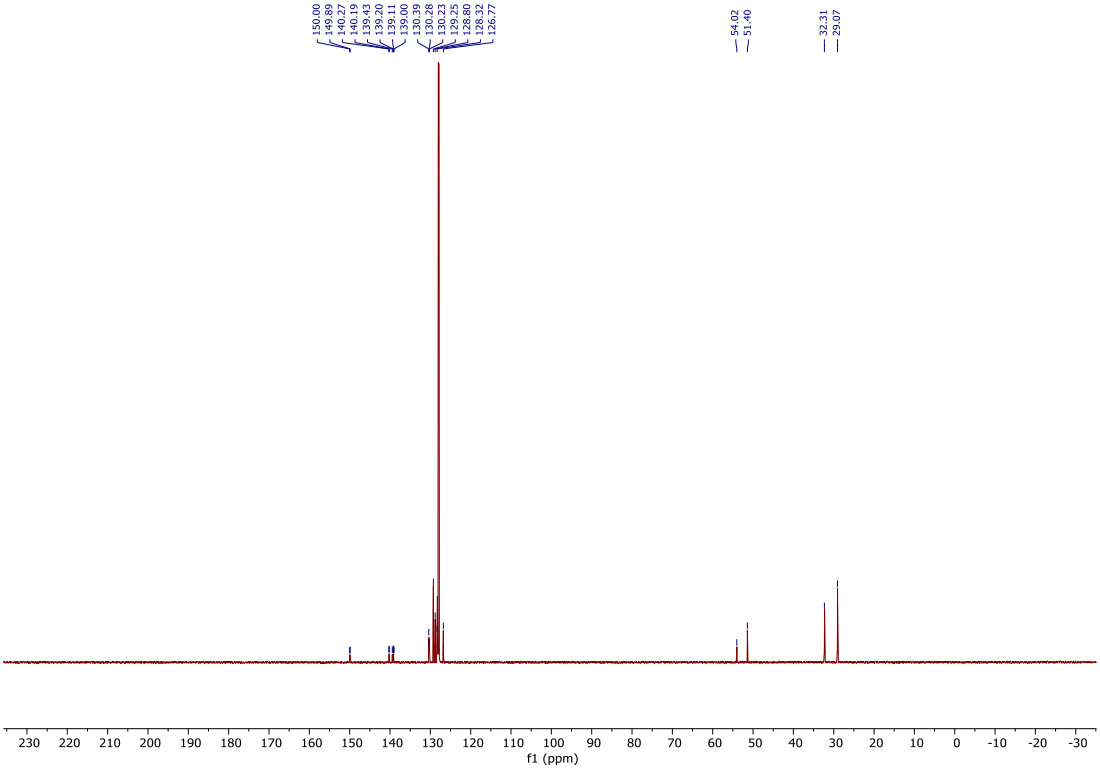


Figure S8. $^{13}$C NMR spectrum of 1,4-bis(2-(ditertbutylamidine)phenyl)benzene (**A**) in $C_6D_6$.

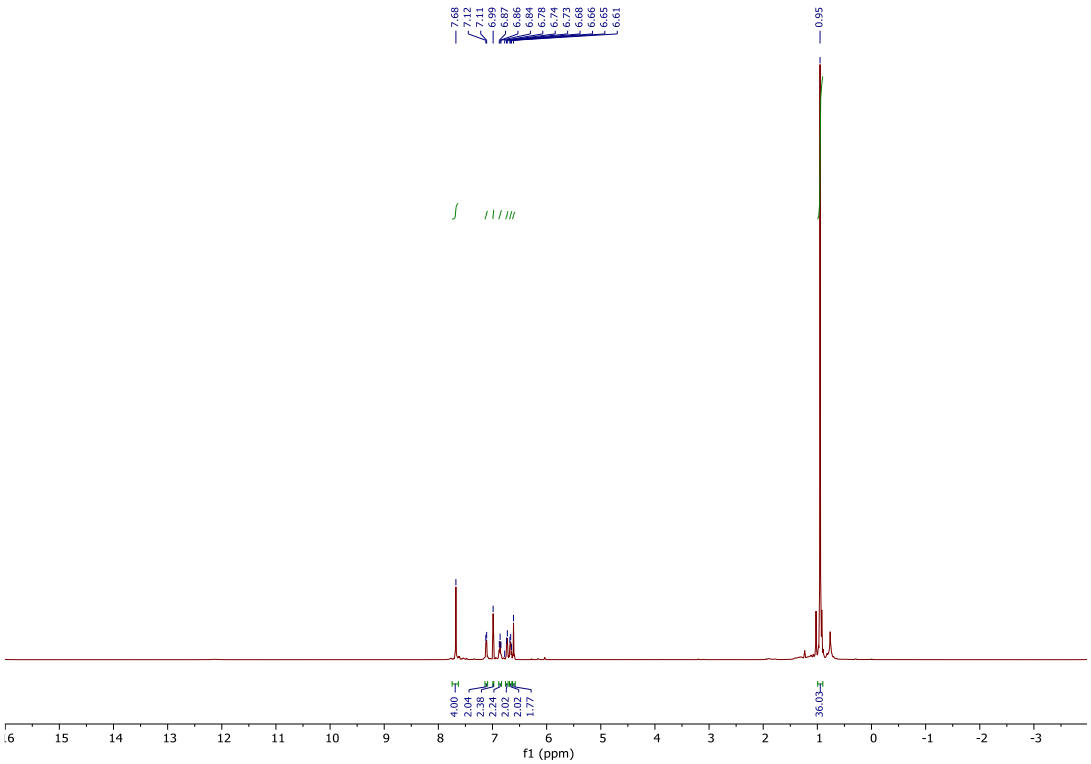


Figure S9. $^{1}$H NMR spectrum of 1,4-bis(2-(ditertbutylamidinate-dichlorosilane)phenyl) benzene (**10**) in $C_6D_6$.

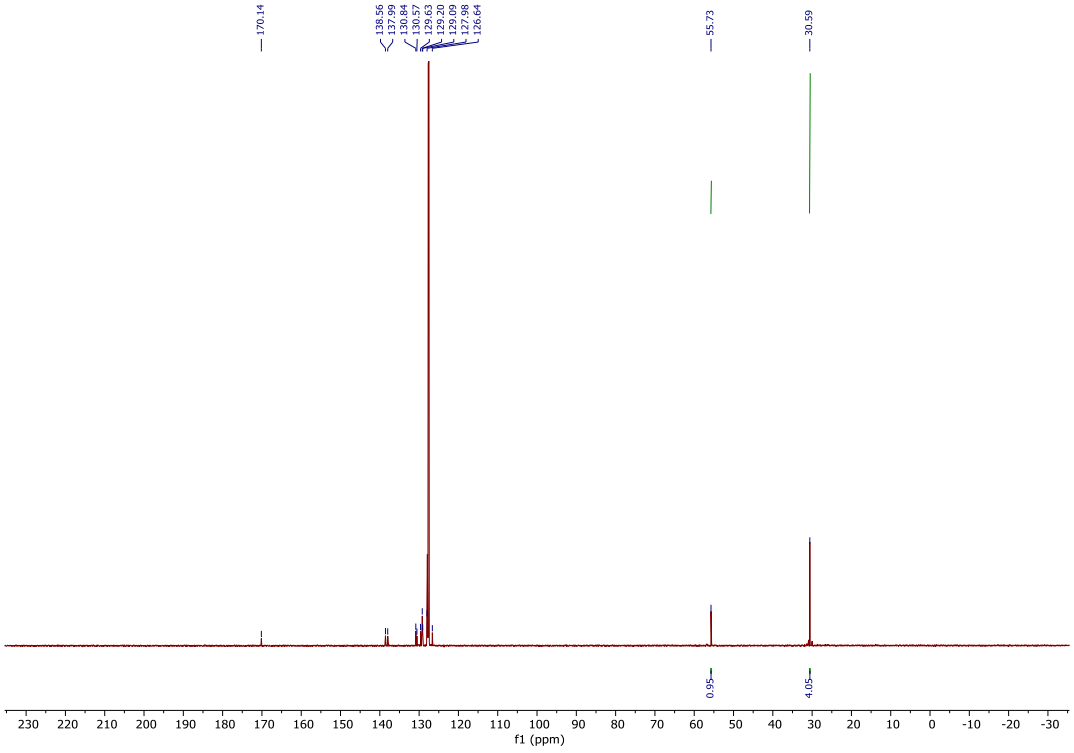


Figure S10. $^{13}$C NMR spectrum of 1,4-bis(2-(ditertbutylamidinate-dichlorosilane)phenyl) benzene (**10**) in $C_6D_6$.

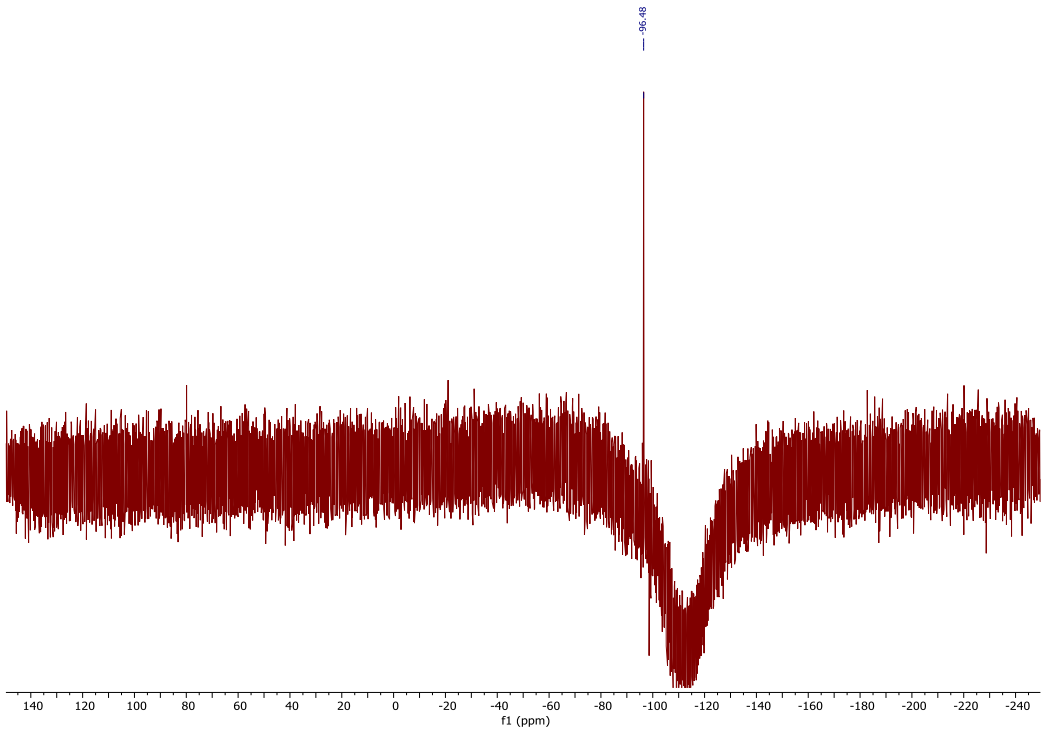


Figure S11. $^{29}Si$ NMR spectrum of 1,4-bis(2-(ditertbutylamidinate-dichlorosilane)phenyl) benzene (**10**) in $C_6D_6$.

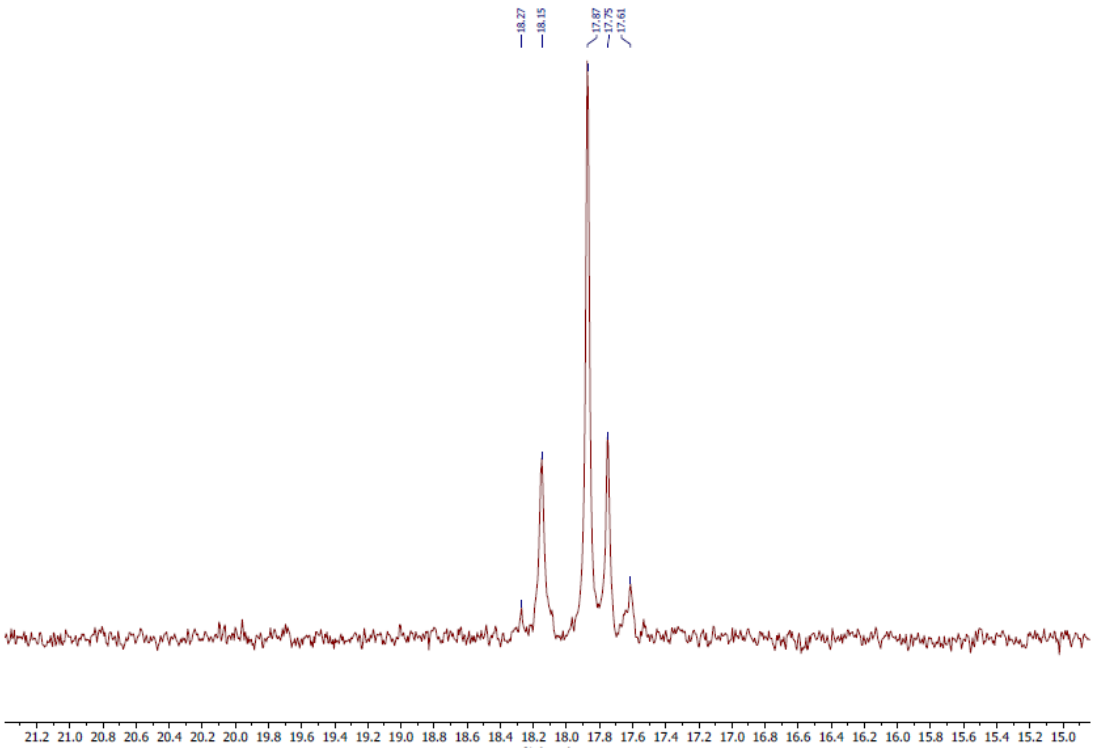


Figure S12 $^{29}Si$ NMR spectrum of the crude mixture from the reaction of compound **10** and two equiavalents of $LiN(SiMe_3)_2$ in $C_6D_6$.

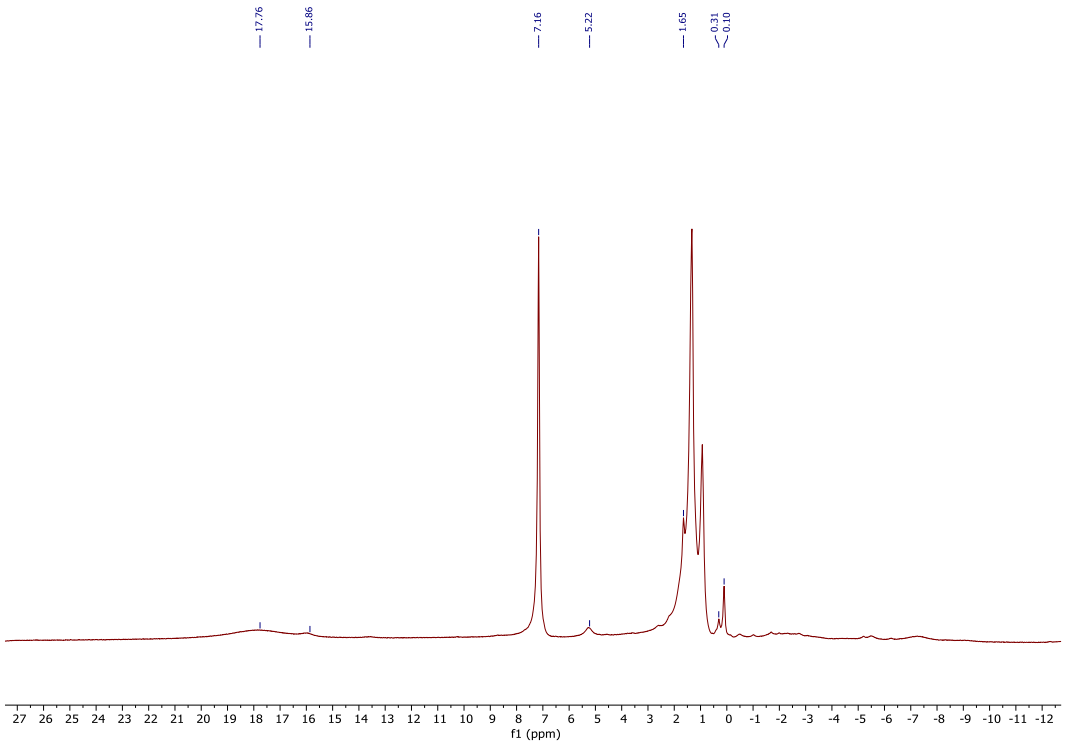


Figure S13. $^{1}$H NMR spectrum of 1,4-bis(2-(ditertbutylamidinate-chlorosilylene Fe{N(SiMe$_3$)$_2$}$_2$)phenyl) benzene (**11**) in $C_6D_6$.

# IR Spectra

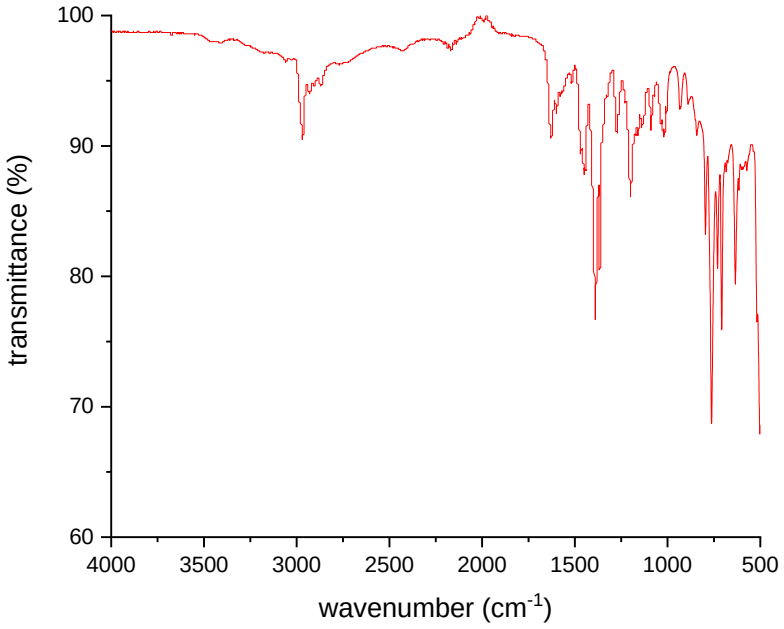


Figure S14. IR Spectrum of $\{PhC(N^tBu)_2SiCl\}_2FeCl_2$ (**3**).

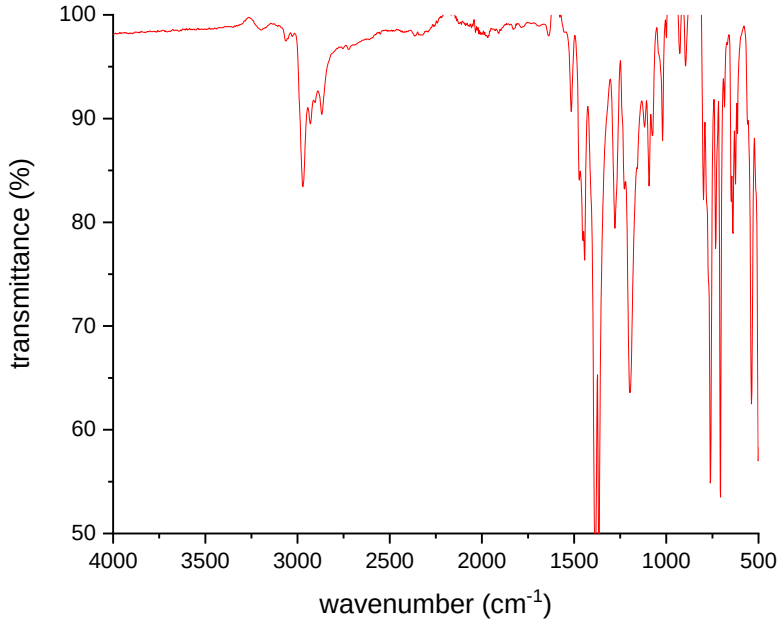


Figure S15. IR Spectrum of $\{PhC(N^tBu)_2SiCl\}_2MnCl_2$ (**4**).

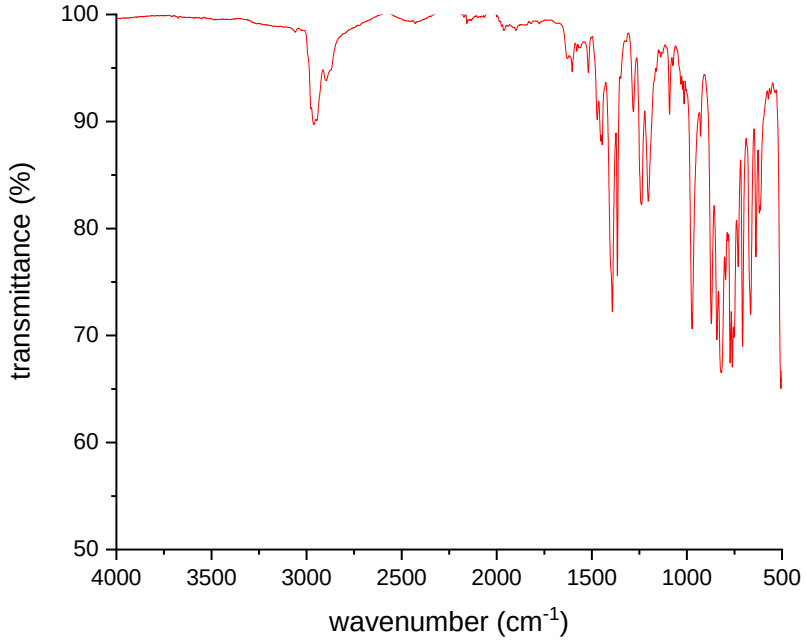


Figure S16. IR Spectrum of [{PhC(N$^t$Bu)$_2$}Si{N(SiMe$_3$)$_2$}CoCl(μ-Cl)]$_2$ (**6**).

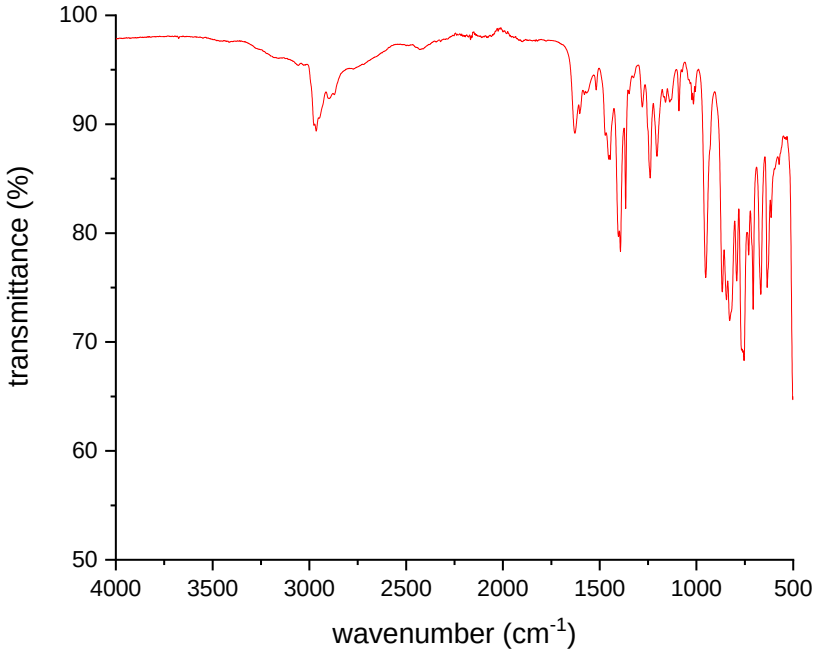


Figure S17. IR Spectrum of [{PhC(N$^t$Bu)$_2$SiCl}Fe{N(SiMe$_3$)$_2$}(μ-Cl)]$_2$ (**7**).

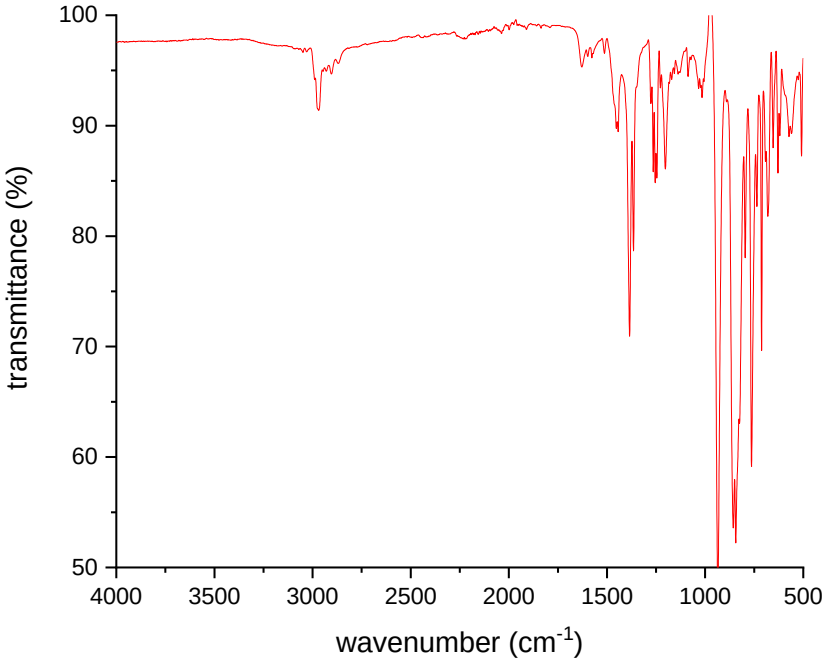


Figure S18. IR Spectrum of [{PhC(N$^t$Bu)$_2$SiCl}Mn{N(SiMe$_3$)$_2$}(μ-Cl)]$_2$ (**8**).

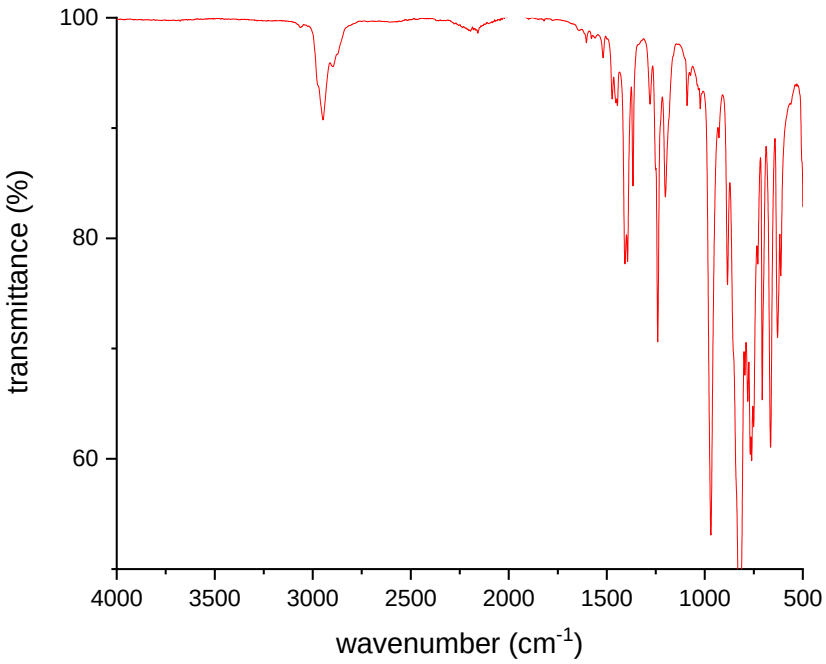


Figure S19. IR Spectrum of {PhC(N$^t$Bu)$_2$SiCl}Fe{N(SiMe$_3$)$_2$}$_2$ (**9**).

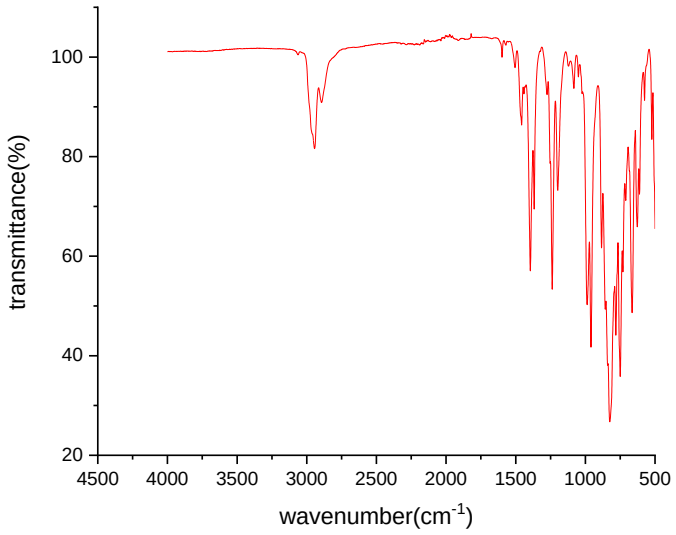


Figure S20 IR Spectrum of 1,4-bis(2-(ditertbutylamidinate-chlorosilylene Fe{N(SiMe$_3$)$_2$}$_2$)phenyl) benzene(**11**).

# X-ray data collection

The crystals of compounds **3**, **4**, **5**, **6**, **7, 8** and **9** were selected for single-crystal X-ray diffraction. Crystals were coated with Paratone-N oil and mounted on a Bruker D8 Venture diffractometer with graphite-monochromatic Mo-Kα radiation (λ = 0.71073 Å). The multi-scan absorption correction was applied by using the SADABS program. Non-hydrogen atoms were refined with anisotropic displacement parameters during the final cycles. All the hydrogen atoms were placed in calculated sites and included as riding atoms with isotropic displacement parameters setting to 1.2 × Ueq of all C (H) groups, all C (H, H) groups and 1.5 × Ueq of all C (H, H, H) groups

**Crystal refinement for (4)**

Compound **4** was found to have disorder of the chloride atoms bound directly to manganese (Cl1 and Cl2). Before modeling the disorder, the Ueq of Cl1 and Cl2 were significantly smaller than Cl3 and Cl4 bound to the silylene ligands. Also, visualization of the residual electron density showed there was a large part of the electron density unaccounted for near Cl1 and Cl2 in our model. We chose to model the disordered chloride ligands Cl1 and Cl2 as a mixture of chloride and bromide. The bromide ligand was chosen because it would account for the higher residual electron density, bromide has the same charge as chloride and has relatively the same size. One potential source of bromide within the structure from our synthesis could be the commercial phenyl lithium that was used in the synthesis of silane **1**. The addition of bromide to the structural model appears to be a much better match than chloride alone. The occupancies of each halide was modeled independently as a mixture of chloride and bromide and refined using the SHELXL

restraint program as the sum of occupancies. The modeled disorder for one of the halides is made up of Cl1 and Br1 with occupancies of 0.453(4) and 0.547(4) respectively. The other mixed halide ligand was made up of Cl2 and Br2 and refined to an occupancy of 0.707(4) and 0.293(4) respectively. Before modeling the disorder $R_1$ = 11.20 % and $wR_2$ = 37.90 %. After modeling the disorder $R_1$ = 4.61 % and $wR_2$ = 10.96 %. A disordered $^t$Bu group of the amidinate portion of the molecule was also disordered and modeled. The disorder was modeled as two parts. Part 1 was composed of C28, C29, and C30 while Part 2 was composed of C31, C32, and C33. The occupancies of part 1 and part 2 were refined using the SHELXL restraint program as the sum of occupancies. Part 1 refined to an occupancy of 0.38(6) while part 2 refined to an occupancy of 0.62(6). Additionally, some distance restraints were used to aid with modeling the disorder.

**Crystal refinement for (8)**

In the case of compound **8**, the three methyl groups of the $^t$Bu group stemming from C12 were disordered. The disorder was modeled as two parts. Part 1 was composed of C131, C132, and C133 while Part 2 was composed of C13, C14, and C15. The occupancies of part 1 and part 2 were refined using the SHELXL restraint program as the sum of occupancies. Part 1 refined to an occupancy of 0.65(3) while part 2 refined to an occupancy of 0.35(3). Additionally, some distance restraints were used to aid with modeling the disorder.

**Crystal refinement for (11)**

Compound **11** was found to have disorder of chloride atoms bond to the silicon atom. The disorder was modeled as six parts. Part 1 was composed of Cl3 and Cl4, part 2 was composed of Cl3A and Cl4A, part 3 was composed of Cl3B and Cl4B. Part 4 was composed of Cl1, part 5 was composed of Cl1A, part 6 was composed of Cl1B. The occupancies of parts 1 (Si2, Cl3, Cl4), 2 (Si2A, Cl3A, Cl4A), and 3 (Si2B, Cl3B, Cl4B) were modeled as $SiCl_2$ units and refined using the SHELXL restraint program as the sum of occupancies. Part 1 refined to an occupancy of 0.299(3), part 2 refined to an occupancy of 0.367(3), part 3 refined to an occupancy of 0.334(3). The other $SiCl_2$ group was modeled as a disordered chloride and occupancies of parts 4 (Cl1), 5 (Cl1A), and 6 (Cl1B) were refined using the SHELXL restraint program as the sum of occupancies. Part 4 refined to an occupancy of 0.797(2), part 5 refined to an occupancy of 0.124(3), part 6 refined to an occupancy of 0.079(3).

Table S1. X-ray data of {PhC(N$^t$Bu)$_2$SiCl}$_2$FeCl$_2$ (**3**).

| | **{PhC(N$^t$Bu)$_2$SiCl}$_2$FeCl$_2$ (3)** |
|---|---|
| **chemical formula** | $C_{30}H_{46}Cl_4FeN_4Si_2$ |
| **fw** | 716.54 |
| ***T* (K)** | 150 |
| ***λ* (Å)** | 0.71073 |
| ***a* (Å)** | 11.4312(7) |
| ***b* (Å)** | 17.2983(12) |
| ***c* (Å)** | 19.8767(16) |
| ***α* (°)** | 90 |
| ***β* (°)** | 105.599(2) |
| ***γ* (°)** | 90 |
| ***V* (Å$^3$)** | 3785.7(5) |
| **space group** | $P2_1$ |
| **Flack Parameter** | 0.099(10) |
| ***Z*, *Z'*** | 4, 2 |
| **$D_{calc}$ (g/cm$^3$)** | 1.257 |
| ***μ* (mm$^{-1}$)** | 0.769 |
| **R1 (I > 2σ(I)), wR2[a]** | 0.0579, 0.1709 |

[a] $R1 = \Sigma||F_o| - |F_c||/\Sigma|F_o|$, $wR2 = (\Sigma[w(F_o^2 - F_c^2)^2]/\Sigma[w(F_o^2)^2])c^{1/2}$

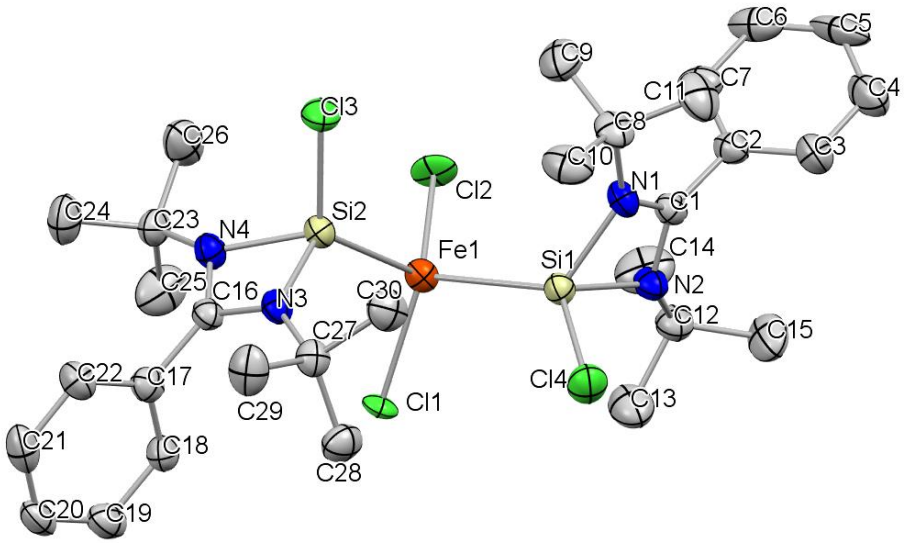


Figure S21. The full numbering scheme of molecule one of {PhC(N$^t$Bu)$_2$SiCl}$_2$FeCl$_2$ (**3**). All atoms shown are depicted with 50% thermal contours. The hydrogen atoms have been removed for clarity.

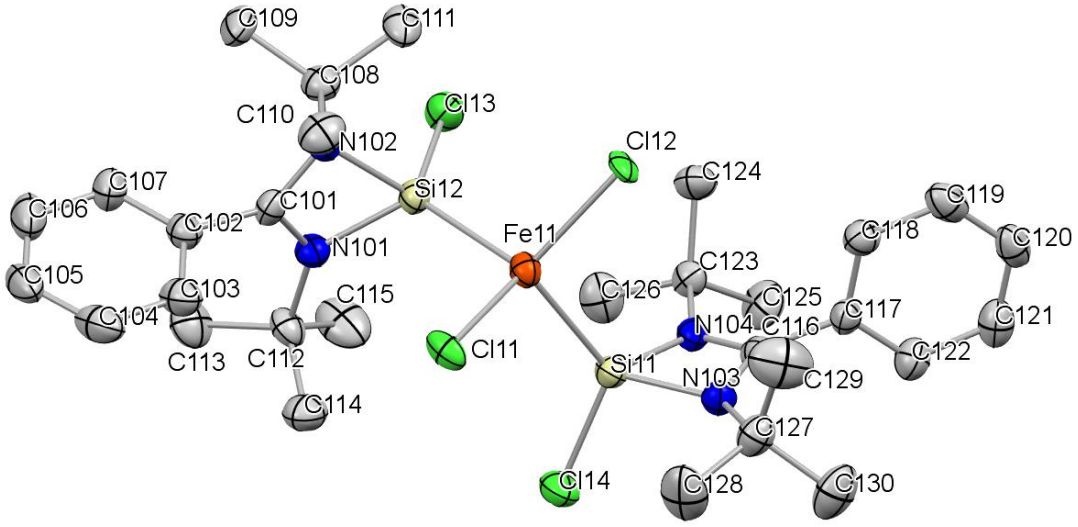


Figure S22. The full numbering scheme of molecule two of $\{PhC(N^tBu)_2SiCl\}_2FeCl_2$ (**3**). All atoms shown are depicted with 50% thermal contours. The hydrogen atoms have been removed for clarity.

Table S2. X-ray data of {PhC(N$^t$Bu)$_2$SiCl}$_2$MnCl$_2$ (**4**).

| | **{PhC(N$^t$Bu)$_2$SiCl}$_2$MnCl$_2$ (4)** |
|---|---|
| **chemical formula** | $C_{30}H_{46}Br_{0.84}Cl_{3.16}MnN_4Si_2$ |
| **fw** | 752.97 |
| ***T* (K)** | 150 |
| ***λ* (Å)** | 0.71073 |
| ***a* (Å)** | 10.5954(9) |
| ***b* (Å)** | 10.9184(8) |
| ***c* (Å)** | 17.2222(14) |
| ***α* (°)** | 77.080(4) |
| ***β* (°)** | 79.212(4) |
| ***γ* (°)** | 73.855(4) |
| ***V* (Å$^3$)** | 1848.6(3) |
| **space group** | $P\bar{1}$ |
| ***Z*, *Z'*** | 2, 1 |
| **$D_{calc}$ (g/cm$^3$)** | 1.353 |
| ***μ* (mm$^{-1}$)** | 1.583 |
| **R1 (I > 2σ(I)), wR2[a]** | 0.0461, 0.1096 |

[a] $R1 = \Sigma||F_o| - |F_c||/\Sigma|F_o|$, $wR2 = (\Sigma[w(F_o^2 - F_c^2)^2]/\Sigma[w(F_o^2)^2])c^{1/2}$

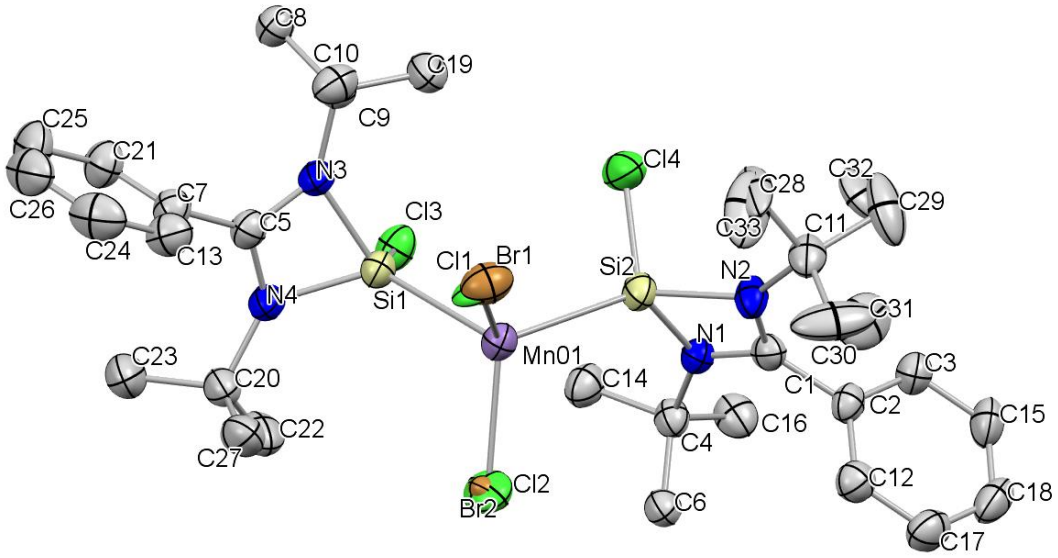


Figure S23. The full numbering scheme of {PhC(N$^t$Bu)$_2$SiCl}$_2$MnCl$_2$ (**4**). All atoms shown are depicted with 50% thermal contours. The hydrogen atoms have been removed for clarity.

Table S3. X-ray data of 2[{PhC(N$^t$Bu)$_2$SiCl}$_2$Co(I)($\eta^6$-C$_6$H$_6$)]$^{2+}$ [Co(II)$_2$Cl$_6$]$^{2-}$ (**5**).

| | **2[{PhC(N$^t$Bu)$_2$SiCl}$_2$Co(I)($\eta^6$-C$_6$H$_6$)]$^{2+}$ [Co(II)$_2$Cl$_6$]$^{2-}$ (5)** |
|---|---|
| **chemical formula** | $C_{36}H_{52}Cl_2CoN_4Si_2$, 0.5($Cl_6Co_2$), 2($C_6H_6$) |
| **fw** | 1048.32 |
| ***T* (K)** | 150 |
| ***λ* (Å)** | 0.71073 |
| ***a* (Å)** | 26.502(2) |
| ***b* (Å)** | 13.2285(9) |
| ***c* (Å)** | 18.1814(15) |
| ***α* (°)** | 90 |
| ***β* (°)** | 117.706(2) |
| ***γ* (°)** | 90 |
| ***V* (Å$^3$)** | 5643.3(8) |
| **space group** | *C*2/*m* |
| ***Z*, *Z'*** | 4, 1 |
| **D$_{calc}$ (g/cm$^3$)** | 1.234 |
| ***μ* (mm$^{-1}$)** | 0.900 |
| **R1 (I > 2σ(I)), wR2[a]** | 0.0740, 0.2481 |

[a] R1 = $\Sigma||F_o| - |F_c||/\Sigma|F_o|$, wR2 = $(\Sigma[w(F_o^2 - F_c^2)^2]/\Sigma[w(F_o^2)^2])c^{1/2}$

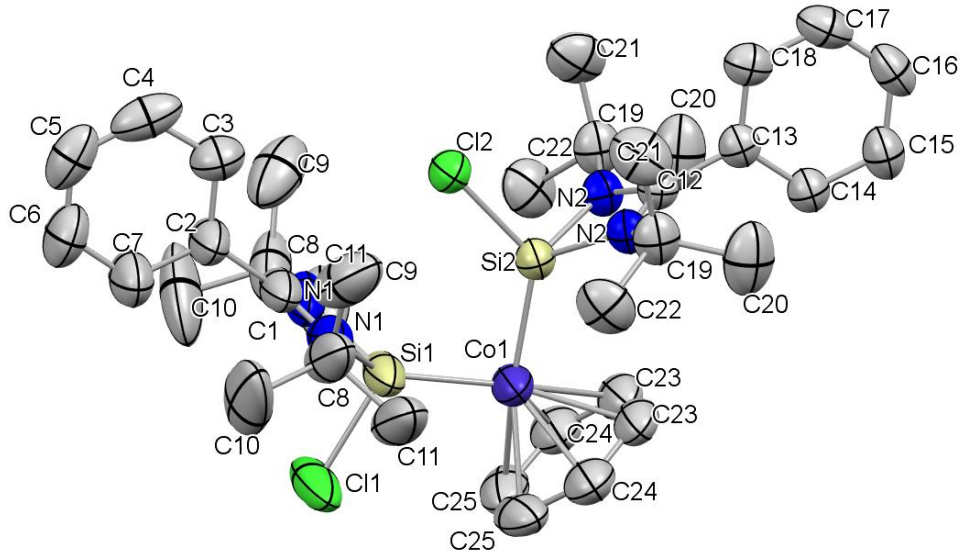


Figure S24. The full numbering scheme of the cation from 2[{PhC(N$^t$Bu)$_2$SiCl}$_2$Co(I)($\eta^6$-C$_6$H$_6$)]$^{2+}$ [Co(II)$_2$Cl$_6$]$^{2-}$ (**5**). All atoms shown are depicted with 50% thermal contours. The hydrogen atoms have been removed for clarity.

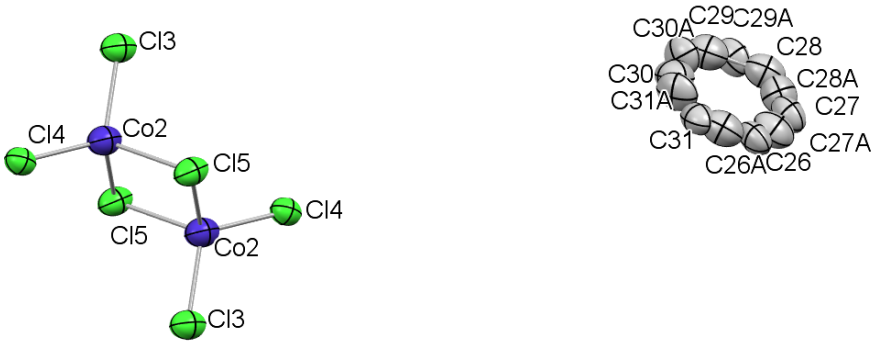


Figure S25. The full numbering scheme of the anion and solvent from 2[{PhC(N$^t$Bu)$_2$SiCl}$_2$Co(I)($\eta^6$-C$_6$H$_6$)]$^{2+}$ [Co(II)$_2$Cl$_6$]$^{2-}$ (**5**). All atoms shown are depicted with 50% thermal contours. The hydrogen atoms have been removed for clarity.

Table S4. X-ray data of [{PhC(N$^t$Bu)$_2$}Si{N(SiMe$_3$)$_2$}CoCl(μ-Cl)]$_2$ (**6**).

| | **[{PhC(N$^t$Bu)$_2$SiN(SiMe$_3$)$_2$}CoCl(μ-Cl)]$_2$ (6)** |
|---|---|
| **chemical formula** | $C_{42}H_{82}Cl_4Co_2N_6Si_6$ |
| **fw** | 1099.34 |
| ***T* (K)** | 150 |
| ***λ* (Å)** | 0.71073 |
| ***a* (Å)** | 10.9455(12) |
| ***b* (Å)** | 14.6642(16) |
| ***c* (Å)** | 18.3130(19) |
| ***α* (°)** | 90 |
| ***β* (°)** | 100.479(3) |
| ***γ* (°)** | 90 |
| ***V* (Å$^3$)** | 2890.3(5) |
| **space group** | $P2_1/c$ |
| ***Z*, *Z'*** | 2, 0.5 |
| **$D_{calc}$ (g/cm$^3$)** | 1.263 |
| ***μ* (mm$^{-1}$)** | 0.916 |
| **R1 (I > 2σ(I)), wR2[a]** | 0.0562, 0.1489 |

[a] $R1 = \Sigma||F_o| - |F_c||/\Sigma|F_o|$, $wR2 = (\Sigma[w(F_o^2 - F_c^2)^2]/\Sigma[w(F_o^2)^2])c^{1/2}$

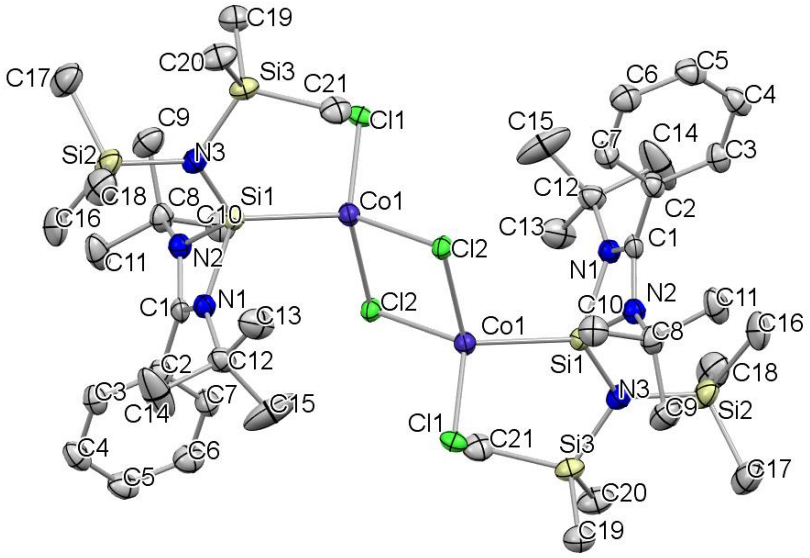


Figure S26. The full numbering scheme of [{PhC(N$^t$Bu)$_2$}Si{N(SiMe$_3$)$_2$}CoCl(μ-Cl)]$_2$ (**6**). All atoms shown are depicted with 50% thermal contours. The hydrogen atoms have been removed for clarity.

Table S5. X-ray data of [{PhC(N$^t$Bu)$_2$}SiCl}Fe{N(SiMe$_3$)$_2$}(μ-Cl)]$_2$ (**7**).

| | **[{PhC(N$^t$Bu)$_2$SiCl}Fe{N(SiMe$_3$)$_2$}(μ-Cl)]$_2$ (7)** |
|---|---|
| **chemical formula** | $C_{42}$ $H_{82}$ $Cl_4$ $Fe_2$ $N_6$ $Si_6$ |
| **fw** | 1093.17 |
| ***T* (K)** | 150 |
| ***λ* (Å)** | 0.71073 |
| ***a* (Å)** | 11.4312(7) |
| ***b* (Å)** | 17.2983(12) |
| ***c* (Å)** | 19.8767(16) |
| ***α* (°)** | 90 |
| ***β* (°)** | 105.599(2) |
| ***γ* (°)** | 90 |
| ***V* (Å$^3$)** | 3785.7(5) |
| **space group** | $P\bar{1}$ |
| ***Z*, *Z'*** | 1, 0.5 |
| **$D_{calc}$ (g/cm$^3$)** | 1.247 |
| ***μ* (mm$^{-1}$)** | 0.838 |
| **R1 (I > 2σ(I)), wR2[a]** | 0.0540, 0.1393 |

[a] $R1 = \Sigma||F_o| - |F_c||/\Sigma|F_o|$, $wR2 = (\Sigma[w(F_o^2 - F_c^2)^2]/\Sigma[w(F_o^2)^2])c^{1/2}$

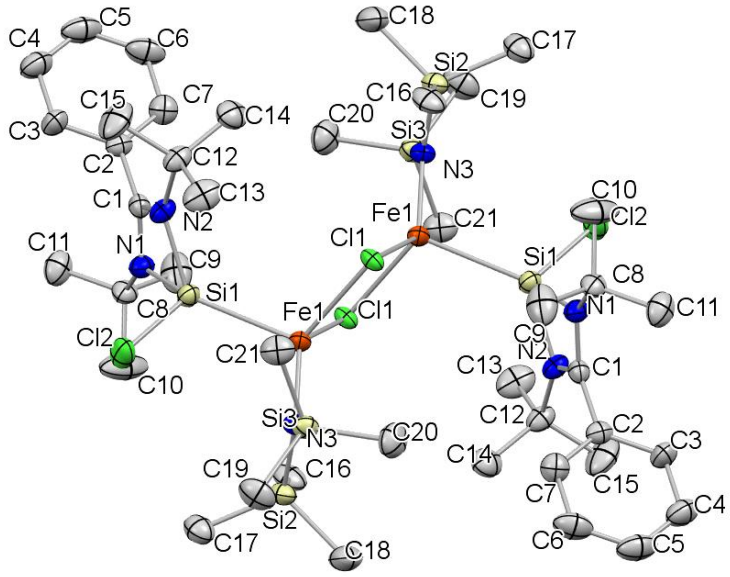


Figure S27. The full numbering scheme of [{PhC(N$^t$Bu)$_2$}SiCl}Fe{N(SiMe$_3$)$_2$}(μ-Cl)]$_2$ (**7**). All atoms shown are depicted with 50% thermal contours. The hydrogen atoms have been removed for clarity.

Table S6. X-ray data of [{PhC(N$^t$Bu)$_2$SiCl}Mn{N(SiMe$_3$)$_2$}(μ-Cl)]$_2$ (**8**).

| | **[{PhC(N$^t$Bu)$_2$SiCl}Mn{N(SiMe$_3$)$_2$}(μ-Cl)]$_2$ (8)** |
|---|---|
| **chemical formula** | $C_{42}H_{82}Cl_4Mn_2N_6Si_6$ |
| **fw** | 1091.36 |
| ***T* (K)** | 150 |
| ***λ* (Å)** | 0.71073 |
| ***a* (Å)** | 14.052(3) |
| ***b* (Å)** | 13.466(2) |
| ***c* (Å)** | 16.318(2) |
| ***α* (°)** | 90 |
| ***β* (°)** | 106.756(6) |
| ***γ* (°)** | 90 |
| ***V* (Å$^3$)** | 2956.7(9) |
| **space group** | $P\bar{1}$ |
| ***Z*, *Z'*** | 2, 0.5 |
| **D$_{calc}$ (g/cm$^3$)** | 1.226 |
| ***μ* (mm$^{-1}$)** | 0.762 |
| **R1 (I > 2σ(I)), wR2[a]** | 0.0669, 0.1937 |

[a] R1 = $\Sigma||F_o| - |F_c||/\Sigma|F_o|$, wR2 = $(\Sigma[w(F_o^2 - F_c^2)^2]/\Sigma[w(F_o^2)^2])c^{1/2}$

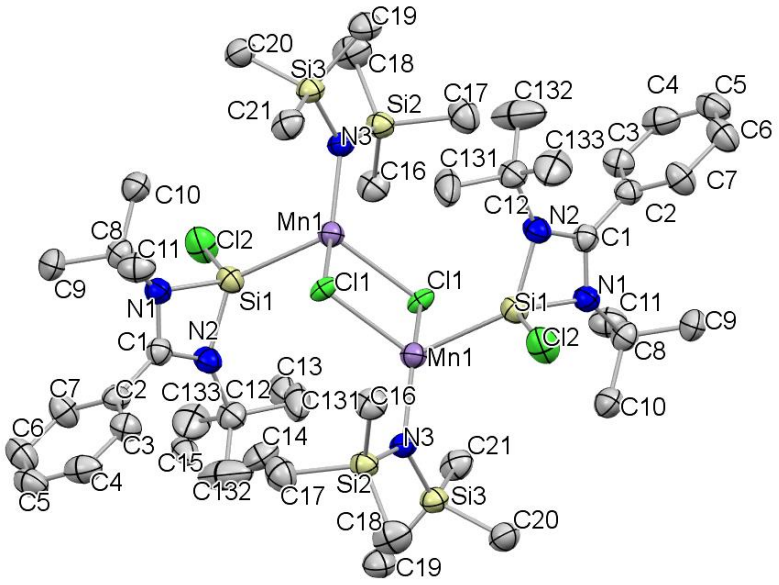


Figure S28. The full numbering scheme of [{PhC(N$^t$Bu)$_2$SiCl}Mn{N(SiMe$_3$)$_2$}(μ-Cl)]$_2$ (**8**). All atoms shown are depicted with 50% thermal contours. The hydrogen atoms have been removed for clarity.

Table S7. X-ray data of {PhC(N$^t$Bu)$_2$SiCl}Fe{N(SiMe$_3$)$_2$}$_2$ (**9**).

| | **{PhC(N$^t$Bu)$_2$SiCl}Fe{N(SiMe$_3$)$_2$}$_2$ (9)** |
|---|---|
| **chemical formula** | $C_{27}H_{59}ClFeN_4Si_5$ |
| **fw** | 716.54 |
| ***T* (K)** | 150 |
| ***λ* (Å)** | 0.71073 |
| ***a* (Å)** | 26.9482(14) |
| ***b* (Å)** | 16.5518(8) |
| ***c* (Å)** | 8.8695(4) |
| ***α* (°)** | 90 |
| ***β* (°)** | 90 |
| ***γ* (°)** | 90 |
| ***V* (Å$^3$)** | 3956.2(3) |
| **space group** | *P*na2$_1$ |
| **Flack Parameter** | 0.045(10) |
| ***Z*, *Z'*** | 4, 1 |
| **D$_{calc}$ (g/cm$^3$)** | 1.128 |
| ***μ* (mm$^{-1}$)** | 0.621 |
| **R1 (I > 2σ(I)), wR2[a]** | 0.0431, 0.1220 |

[a] $R1 = \Sigma||F_o| - |F_c||/\Sigma|F_o|$, $wR2 = (\Sigma[w(F_o^2 - F_c^2)^2]/\Sigma[w(F_o^2)^2])c^{1/2}$

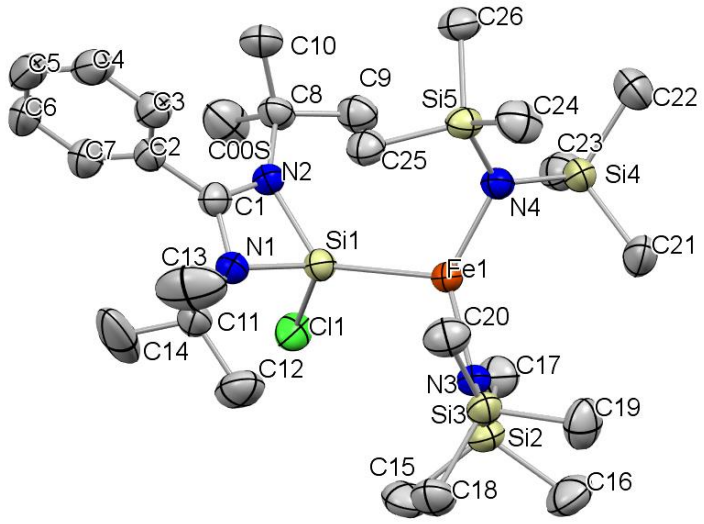


Figure S29. The full numbering scheme of {PhC(N$^t$Bu)$_2$SiCl}Fe{N(SiMe$_3$)$_2$}$_2$ (**9**). All atoms shown are depicted with 50% thermal contours. The hydrogen atoms have been removed for clarity.

Table S8. X-ray data of 1,4-bis(2-(ditertbutylamidine)phenyl)benzene (**A**).

| | **1,4-bis(2-(ditertbutylamidine)phenyl)benzene (A)** |
|---|---|
| **chemical formula** | $C_{36}H_{52}N_4$ |
| **fw** | 716.54 |
| ***T* (K)** | 150 |
| ***λ* (Å)** | 0.71073 |
| ***a* (Å)** | 7.7897(4) |
| ***b* (Å)** | 27.7273(18) |
| ***c* (Å)** | 7.9686(5) |
| ***α* (°)** | 90 |
| ***β* (°)** | 104.039(2) |
| ***γ* (°)** | 90 |
| ***V* (Å$^3$)** | 1669.71(17) |
| **space group** | $P2_1/n$ |
| ***Z*, *Z'*** | 2, 0.5 |
| **$D_{calc}$ (g/cm$^3$)** | 1.076 |
| ***μ* (mm$^{-1}$)** | 0.621 |
| **R1 (I > 2σ(I)), wR2[a]** | 0.0508, 0.1361 |

[a] $R1 = \Sigma||F_o| - |F_c||/\Sigma|F_o|$, $wR2 = (\Sigma[w(F_o^2 - F_c^2)^2]/\Sigma[w(F_o^2)^2])c^{1/2}$

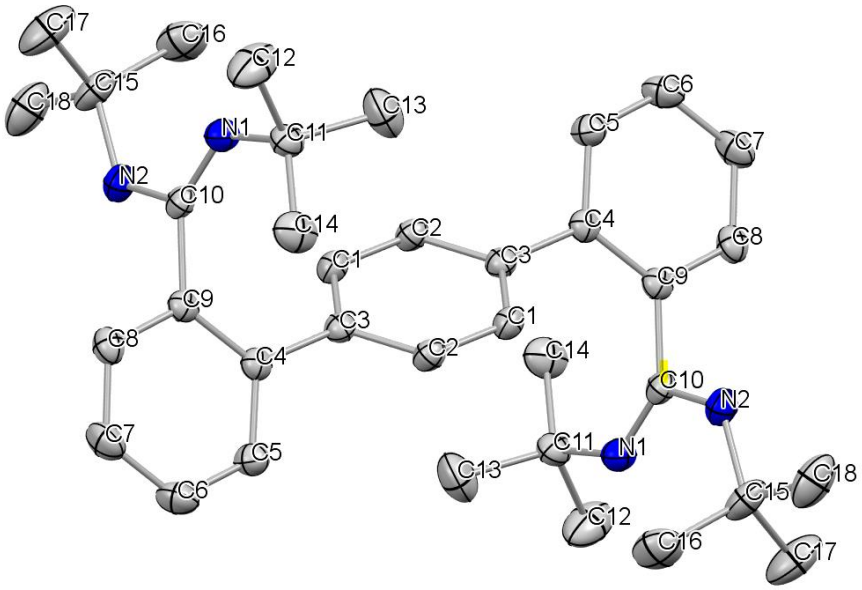


Figure S30. The full numbering scheme of 1,4-bis(2-(ditertbutylamidine)phenyl)benzene (**A**)**.** All atoms shown are depicted with 50% thermal contours. The hydrogen atoms have been removed for clarity.

Table S9. X-ray data of 1,4-bis(2-(ditertbutylamidinate-dichlorosilane)phenyl) benzene (**10**).

| | **1,4-bis(2-(ditertbutylamidinate-dichlorosilane)phenyl) benzene (10)** |
|---|---|
| **chemical formula** | $C_{43}H_{56}N_4Cl_4Si_2$ |
| **fw** | 826.90 |
| ***T* (K)** | 150 |
| ***λ* (Å)** | 0.71073 |
| ***a* (Å)** | 11.9514(9) |
| ***b* (Å)** | 19.3184(16) |
| ***c* (Å)** | 19.1714(17) |
| ***α* (°)** | 90 |
| ***β* (°)** | 91.199(2) |
| ***γ* (°)** | 90 |
| ***V* (Å$^3$)** | 4425.4(6) |
| **space group** | $P2_1/n$ |
| ***Z*, *Z'*** | 4, 1 |
| **$D_{calc}$ (g/cm$^3$)** | 1.241 |
| ***μ* (mm$^{-1}$)** | 0.356 |
| **R1 (I > 2σ(I)), wR2[a]** | 0.0989, 0.2012 |

[a] $R1 = \Sigma||F_o| - |F_c||/\Sigma|F_o|$, $wR2 = (\Sigma[w(F_o^2 - F_c^2)^2]/\Sigma[w(F_o^2)^2])c^{1/2}$

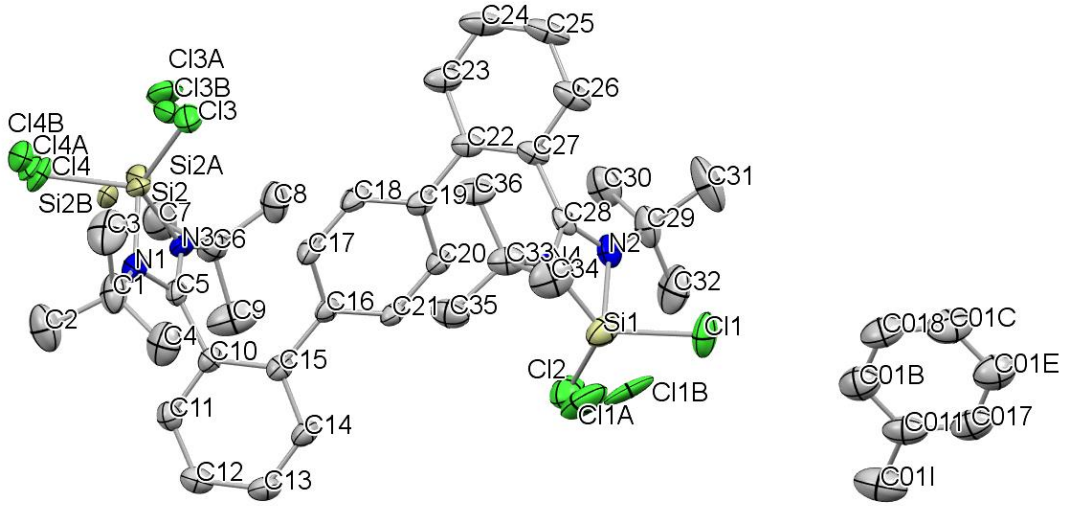


Figure S31. The full numbering scheme of 1,4-bis(2-(ditertbutylamidinate-dichlorosilane)phenyl) benzene (**10**). All atoms shown are depicted with 50% thermal contours. The hydrogen atoms have been removed for clarity.

Table S10. X-ray data of 1,4-bis(2-(ditertbutylamidinate-chlorosilylene Fe{N(SiMe$_3$)$_2$}$_2$)phenyl) benzene (**11**).

| | **1,4-bis(2-(ditertbutylamidinate-chlorosilylene Fe{N(SiMe$_3$)$_2$}$_2$)phenyl) benzene (11)** |
|---|---|
| **chemical formula** | $C_{60}H_{120}N_8Cl_2Si_{10}Fe_2$ |
| **fw** | 1417.14 |
| ***T* (K)** | 150 |
| ***λ* (Å)** | 1.54178 |
| ***a* (Å)** | 37.0728(13) |
| ***b* (Å)** | 13.2937(5) |
| ***c* (Å)** | 17.4231(6) |
| ***α* (°)** | 90 |
| ***β* (°)** | 110.472(1) |
| ***γ* (°)** | 90 |
| ***V* (Å$^3$)** | 8044.4(5) |
| **space group** | *C*2/*c* |
| ***Z*, *Z'*** | 4, 0.5 |
| **D$_{calc}$ (g/cm$^3$)** | 1.170 |
| ***μ* (mm$^{-1}$)** | 5.223 |
| **R1 (I > 2σ(I)), wR2[a]** | 0.0415, 0.1190 |

[a] $R1 = \Sigma||F_o| - |F_c||/\Sigma|F_o|$, $wR2 = (\Sigma[w(F_o^2 - F_c^2)^2]/\Sigma[w(F_o^2)^2])c^{1/2}$

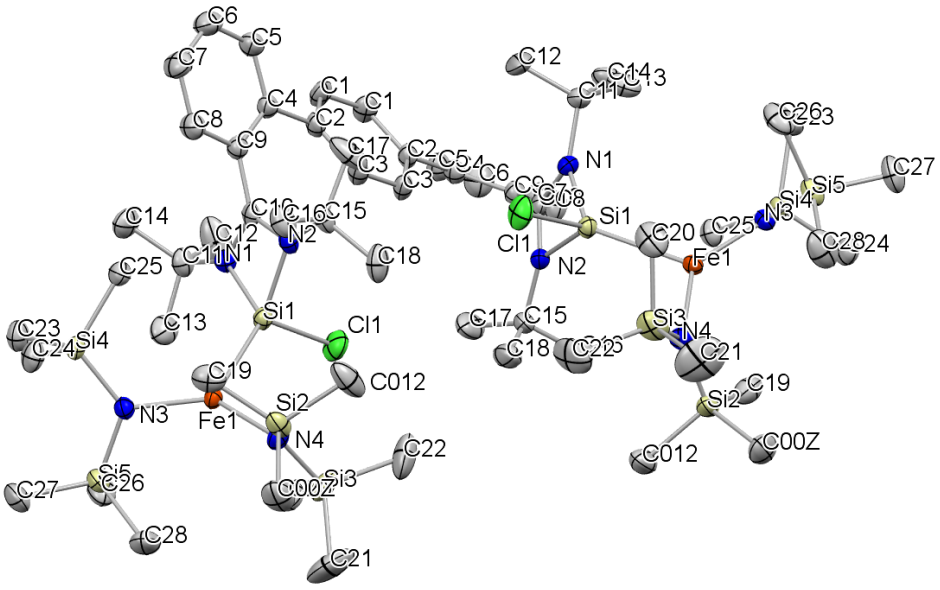


Figure S32. The full numbering scheme of 1,4-bis(2-(ditertbutylamidinate-chlorosilylene Fe{N(SiMe$_3$)$_2$}$_2$)phenyl) benzene (**11**). All atoms shown are depicted with 50% thermal contours. The hydrogen atoms have been removed for clarity.

# Supplementary References


1. S. S. Sen, H. W. Roesky, D. Stern, J. Henn and D. Stalke, *J. Am. Chem. Soc.*, 2010, **132**, 1123-1126.
2. D. L. Broere, I. Coric, A. Brosnahan and P. L. Holland, *Inorg. Chem.*, 2017, **56**, 3140-3143.
3. A. M. Bryan, G. J. Long, F. Grandjean and P. P. Power, *Inorg. Chem.*, 2013, **52**, 12152-12160.
4. A. Eichhöfer and S. Lebedkin, *Inorg. Chem.*, 2018, **57**, 602-608.
5. A. Velian, S. Lin, A. J. M. Miller, M. W. Day and T. Agapie, *J. Am. Chem. Soc.*, 2010, **132**, 6296-6297.
6. S. K. Sur, *Journal of Magnetic Resonance (1969)*, 1989, **82**, 169-173.
7. D. F. Evans, *J. Chem. Soc.*, 1959, 2003-2005.
8. J. Wu, W. Dai, J. H. Farnaby, N. Hazari, J. J. Le Roy, V. Mereacre, M. Murugesu, A. K. Powell and M. K. Takase, *Dalton Trans.*, 2013, **42**, 7404-7413.
9. D. Gallego, S. Inoue, B. Blom and M. Driess, *Organometallics*, 2014, **33**, 6885-6897.
10. P. P. Samuel, K. C. Mondal, N. Amin Sk, H. W. Roesky, E. Carl, R. Neufeld, D. Stalke, S. Demeshko, F. Meyer, L. Ungur, L. F. Chibotaru, J. Christian, V. Ramachandran, J. van Tol and N. S. Dalal, *J. Am. Chem. Soc.*, 2014, **136**, 11964-11971.
11. O. V. Dolomanov, L. J. Bourhis, R. J. Gildea, J. A. K. Howard and H. Puschmann, *J. Appl. Crystallogr.*, 2009, **42**, 339-341.
12. G. Sheldrick, *Acta Cryst. A*, 2015, **71**, 3-8.
13. G. Sheldrick, *Acta Cryst. A*, 2008, **64**, 112-122.